

# Stellar evolution with rotation

## I. The computational method and the inhibiting effect of the $\mu$ -gradient

Georges Meynet and André Maeder

Geneva Observatory, CH-1290 Sauverny, Switzerland

Received 30 January 1996 / Accepted 21 May 1996

**Abstract.** We study the effects of rotation on the structure and evolution of massive stars. The method of Kippenhahn & Thomas (1970) to incorporate the hydrostatic effects of rotation in one dimensional stellar evolutionary codes is strictly valid only in case the angular velocity distribution has a cylindrical symmetry. We demonstrate how this method can be applied (cf. Appendix) in the case where the angular velocity is constant on isobars (“shellular rotation law”, cf. Zahn 1992). We also investigate the structural effects of rotation on the stellar atmosphere. The effects of rotational mixing are considered with the theory of Zahn (1992) for the circulation and turbulence in rotating stars. We suppose that the angular momentum in a given shell remains constant with time (asymptotic regime). The subsequent developments brought to the Richardson criterion by Maeder (1995a) and Maeder and Meynet (1996) to account for thermal effects on the shear instability are also applied.

Evolutionary tracks are calculated for initial masses of 9, 20, 40 and 60  $M_{\odot}$  with account of the above hydrostatic and mixing effects. The main results are the following ones:

1) The hydrostatic effects alone are quite modest: when the initial angular velocity ( $\Omega$ ) increases from 0 to 90% of the surface critical velocity ( $\Omega_{\text{crit}}$ ), the lifetimes of massive star models (40 to 60  $M_{\odot}$ ) are increased by 1 to 2%. The evolutionary tracks are shifted towards lower luminosities, making them appear as the ones resulting from slightly lower initial mass stars, typically 0.5 to 2.5  $M_{\odot}$  smaller.

2) Surprisingly we find that the  $\mu$ -gradients, when non zero, are always strong enough to inhibit mixing. Indeed, the effects of  $\mu$ -gradients are quite difficult to overcome and this tends to make the rotationally induced mixing inoperant when the Richardson criterion is applied.

3) We suggest that different mixing criteria and/or diffusion coefficients must be searched for and applied if one wants to reproduce the observations by Herrero et al. (1992). Indeed these authors show that above a certain rotational velocity, quite efficient mixing processes are active and able to modify the surface abundances in helium during a fraction of the main sequence lifetime.

**Key words:** instabilities – turbulence – methods: numerical – stars: early-type – evolution – rotation

---

### 1. Introduction

There are at least three main reasons to reconsider at the present time the problem of the effects of rotation on stellar structure and evolution:

1) The recent finding of Herrero et al. (1992) that all fast rotators among O-stars show surface He-enrichments points towards the existence of very efficient mixing processes induced by rotation. Indeed in these stars, mixing is strong enough to transport to the surface the newly processed elements during a fraction of the main sequence lifetime. The next generation of stellar models should be able to account for such observations.

2) A number of discrepancies between models and observations still exist and they generally point in favor of more mixing processes in the models (Maeder, 1995b, see also the references therein). Without going into the details let us briefly mention some of them below:

- Extended cluster main sequences (see *e.g.* Maeder & Meynet 1989).
- $N/C$  and  $^{13}C/^{12}C$  enrichments on the Red Giant Branch (see *e.g.* Charbonnel 1994, 1995).
- Abundances in AGB stars (see *e.g.* Mowlavi 1995).
- He discrepancy in O-stars (Herrero et al. 1992).
- He- and N-excesses in OBA supergiants and in SN 1987 A (Walborn 1976; Fransson et al. 1989; Venn 1995ab, Venn et al. 1996).
- The blue Hertzsprung gap (Fitzpatrick & Garmany 1990).
- The ratio of the number of blue to red supergiants in galaxies (Langer & Maeder 1995).
- Existence of stars with characteristics intermediate between WN and WC stars (Langer 1991).
- The apparent necessity to account for some primary nitrogen production in massive stars (see *e.g.* Dahmen et al. 1995; Kunth et al. 1995).

Of course we do not claim here that all these differences between theory and observation will be resolved by the inclusion of the effects of rotation into the stellar models. However to go ahead, a first step is to better understand and quantify these effects which can deeply modify stellar evolution.

3) Finally the theory of the transport mechanisms induced by rotation has been considerably improved by Zahn (1992) who studied in details the interaction between meridian circulation and turbulence in rotating stars. He has established in a coherent way the equations governing both the transport of the chemical species and of the angular momentum. In his theory the sole a priori assumption is that the horizontal turbulence is much stronger than the vertical one. This conjecture leads to an internal “shellular” rotation law in agreement with the one deduced in the sun from the study of the acoustic waves (Tomczyk et al. 1995).

With in hands, observations which can serve as a check of our model building, and a theory which for the first time couples in a consistent manner the transport of angular momentum and that of the chemical species, we are now in a good position to address the problem of the effects of rotation on stellar evolution.

## 2. The rotating stellar models

### 2.1. The computational method

Rotation may affect the equations of stellar structure in four ways (cf e.g. Endal & Sofia 1976) :

1. Centrifugal forces reduce the effective gravity at any point not on the axis of rotation.
2. Since the centrifugal force is not, in general, parallel to the force of gravity, equipotential surfaces are no longer spheres.
3. Because the radiative flux varies with the local effective gravity (the von Zeipel effect, 1924), the radiative flux is not constant on an equipotential surface.
4. Rotation may induce some mixing processes.

In the present models, we consider these four effects.

In general, to incorporate into the stellar structure equations, the effects of rotation, the method devised by Kippenhahn & Thomas (1970) is used (see e.g. Endal & Sofia 1976; Pinsonneault et al. 1990; Fliegner & Langer 1995; Chaboyer et al. 1995). The main idea of this method is to replace the spherical stratification which prevails in non rotating stars by a rotationally deformed stratification. The problem can be kept one dimensional in the case where the effective gravity (*i.e.* the gravity decreased by the effect of the centrifugal force) can be derived from a potential (conservative case). Indeed, in this case the pressure  $P$  and the density  $\rho$  keep a constant value on an equipotential. The temperature  $T$  remains also constant if the chemical composition is homogeneous on equipotentials. Thus in a rotating star, the stellar structure equations almost keep the same form as in a non rotating star if they are written on equipotentials

It is quite straightforward to introduce this procedure into a stellar evolutionary code. Unfortunately it applies only in the

case a conservative potential exists *i.e.* in case a cylindrical symmetry for the angular velocity distribution prevails (Poincaré-Wavre theorem, see Tassoul 1978). As already stated in the introduction above, the theory of Zahn (1992) assumes that turbulence is anisotropic, with a stronger transport in the horizontal directions than in the vertical one. This enforces a rotation rate which, to first approximation, remains constant on isobar (“shellular” rotation). Obviously such a rotation law does not fall into the conservative case and the Kippenhahn & Thomas method cannot be used. In the Appendix, we show however that it is possible to adapt the Kippenhahn & Thomas method to the case of a “shellular” rotation law and we describe in details the way we have implemented the effects of shellular rotation in the stellar structure equations.

### 2.2. The physical ingredients

The solar initial chemical composition (mass fraction of the heavy elements  $Z = 0.020$ ), the nuclear reaction rates, the mass loss rates are as in the previous grids of stellar models from the Geneva group (see Schaller et al. 1992). The new OPAL radiative opacities from Iglesias & Rogers (1993) are used, complemented at temperatures below 6000 K with the atomic and molecular opacities by Kurucz (1991).

We considered the Ledoux criterion for convection without semiconvective diffusion. Let us emphasize here that the main conclusion of this paper concerning the inhibiting effect of the molecular weight gradient is not depending on this particular choice (see section 4).

In rotating stars some mixing is expected caused by the meridian circulation (Eddington 1925, 1926; Vogt 1925). This mixing process not only transports the chemical species but also advects angular momentum, the conservation of which induces differential rotation. In the nearly inviscid stellar material, turbulent motion will appear as a result of various instabilities produced by differential rotation. Among these instabilities, the shear instability plays certainly the most important role (Spiegel & Zahn 1970; Zahn 1974, 1975). We have thus the following logical links between these various effects: rotation implies meridian circulation, which in turn implies differential rotation which produces shear instabilities. How the shear instability will interact with the meridian circulation pattern is not an easy problem. The main difficulty comes from the impossibility to describe from first principles the properties of the turbulent motions sustained by the shear. However Zahn (1992), starting from the unique and reasonable assumption that the turbulence is more vigorous in the horizontal direction than in the vertical one, succeeded in establishing in a coherent way the equations for the transport of the chemical species and of the angular momentum resulting from these hydrodynamical processes. Let us note here that the above conjecture on the anisotropy of the turbulence leads to a “shellular rotation law” which seems to be realised in the interior of the Sun (Tomczyk et al. 1995).

Following Zahn (1992), the transport of the chemical species is treated with a diffusion equation. The diffusion coefficient is composed of two terms: a term  $D_{\text{shear}}$  accounting for the

effects of the vertical turbulence induced by the shear and a term  $D_{\text{eff}}$  describing the concomitant effects of the circulation and of the horizontal turbulence induced by the shear. Turbulent motions are sustained when the Reynolds number  $Re = lv/\nu$  is above a critical value  $Re_c$ , of the order of 3000 ( $l$  is the characteristic size of an eddy,  $v$  its velocity and  $\nu$  the viscosity). For current inner conditions in massive stars, this requirement is generally fulfilled (Maeder & Meynet 1996). More constraining is the Richardson criterion (see Chandrasekhar 1961) which may completely suppress the effects of shear mixing. Indeed, this criterion states that a sufficient condition for stability (*i.e.* for no mixing) is that the Richardson number be superior to 1/4. As we shall see below, this Richardson criterion plays an important role in deciding which region of a star can or cannot be mixed by rotational turbulence. Generally this stability criterion is fulfilled in stellar regions where there is a molecular weight gradient ( $\mu$ -gradient), even quite modest, and thus no mixing occurs. However the Richardson criterion as it is classically given (see *e.g.* Zahn 1992) needs some modifications in order to take into account:

- 1) In a more consistent way the radiative losses and the vertical  $\mu$ -gradients.
- 2) The coupling between the shears and their effects on the T-gradient.
- 3) The diffusion both in the radiative and semiconvective zones.

Maeder (1995a) has established the Richardson criterion taking into account the effects indicated on point 1). Maeder & Meynet (1996) have pursued its improvement by considering points 2) and 3). In this paper we shall consider the Richardson criterion and the associated diffusion coefficient  $D_{\text{shear}}$  as they have been established by these last authors. It can be expressed as

$$D_{\text{shear}} = 2K\Gamma_{\text{max}},$$

where  $K$  is the thermal diffusivity and  $\Gamma_{\text{max}}$  is the maximum Peclet number (divided by a factor 6) of the turbulent eddies.  $D_{\text{eff}}$  is related to  $D_{\text{shear}}$  and to the angular velocity gradient  $\frac{d \ln \Omega}{dr}$  through the expression:

$$D_{\text{eff}} = \frac{1}{30} \frac{rU^2}{|2V - \alpha U|},$$

with

$$U = -5D_{\text{shear}} \frac{d \ln \Omega}{dr}.$$

We consider here the case of “no wind” described by Zahn (1992, see this reference for the meaning of the other variables and for a thorough discussion of these expressions).

For massive stars and for asymptotic regime (see Zahn, 1992), the advection of angular momentum by the meridional currents are compensated by the diffusion of angular momentum through shear flow. In this case one can consider that the angular momentum in a given shell remains constant with time (see Appendix A.4 for the expression of the specific angular momentum). We shall further discuss the consequences of this simplifying assumption.

### 3. Hydrostatic effects of rotation

By hydrostatic effects of rotation we mean here the influence on the stellar structure of the centrifugal force, letting aside the effects produced by the transport mechanisms induced by rotation. Such hydrostatic effects have been already studied by numerous authors in the past (Faulkner et al. 1968; Kippenhahn et al. 1970; Kippenhahn & Thomas 1970; Sackmann 1970; Endal & Sofia 1976; Kippenhahn 1977). However it appears interesting to briefly consider them in this paper in order to estimate, in the frame of the “shellular” stellar models, the importance of these hydrostatic effects with respect to the transport processes, and to up-date with modern physical ingredients the results obtained by previous works.

#### 3.1. Effects of rotation on the ZAMS

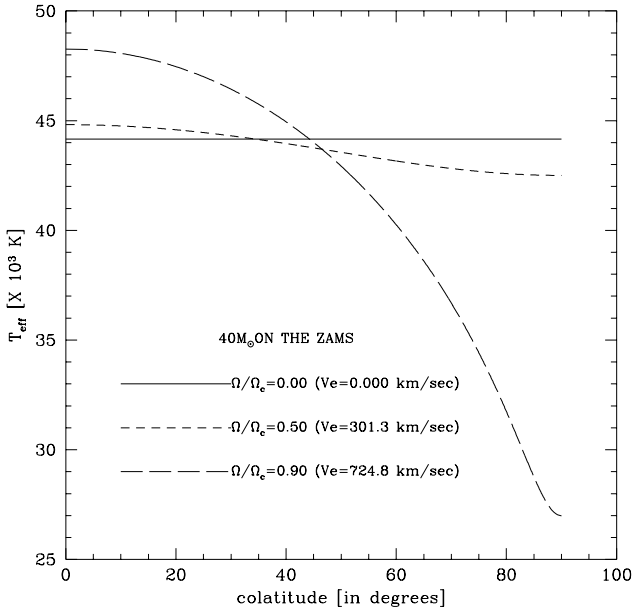
As starting models, we considered uniformly rotating models on the zero age main sequence (ZAMS). Some characteristics of these models are given in Table 1 as a function of the initial mass and angular velocity: in column 2 are listed the ratios of the angular velocity to the critical velocity ( $\Omega_{\text{crit}}$  corresponds to the breaking equatorial velocity at the surface on the ZAMS), the equatorial velocities  $V_{\text{eq}}$  and the positions in the theoretical HR diagram are indicated in columns 3 to 5, the oblatenesses (polar radius over the equatorial radius  $R_p(\Omega)/R_e(\Omega)$ ) and the ratios between the equatorial radius obtained with rotation and that obtained without rotation ( $R_e(\Omega)/R_e(\Omega = 0)$ ) are given in columns 6 and 7 respectively.

The effective temperatures listed in Table 1 have a different meaning than usual in the sense that they represent some kind of a mean effective temperature of the star. Let us recall that at the surface of a rotating star, the flux (and therefore the effective temperature) is proportional to the local effective gravity (theorem of Von Zeipel 1924). To illustrate this point we have plotted on Fig. 1 the variations of the local effective temperature with the colatitude at the surface of rotating  $40 M_{\odot}$  ZAMS models, using the relation given by Maeder (1971). At 90% of the critical angular velocity, the polar regions have  $T_{\text{eff}}$  enhanced by  $\sim 1.8$  with respect to temperatures of the equatorial zones. In order to associate only one representative value of the effective temperature to each of our stellar models, we have used the relation  $L = S\sigma T_{\text{eff}}^4$  where  $L$  is the luminosity,  $S$  the rotationally deformed stellar surface,  $\sigma$  the Stefan-Boltzmann constant and  $T_{\text{eff}}$  the effective temperature (see also Appendix A.3).

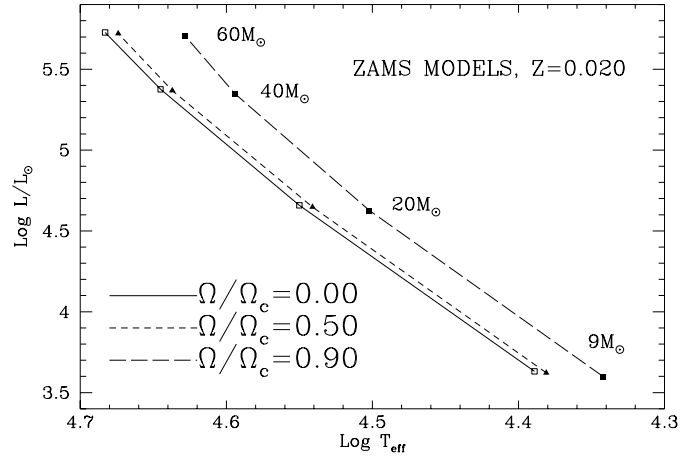
From Table 1, one can see that the effects of rotation on the hydrostatic structure are modest. Fig. 2 presents the ZAMS we have obtained in the theoretical HR diagram. As was found by Kippenhahn & Thomas (1970), rotation provokes a decrease of the luminosity and of the effective temperature. These decreases are quite modest (2% for  $\Omega/\Omega_{\text{crit}} = 0.5$ , between 5 and 11% for  $\Omega/\Omega_{\text{crit}} = 0.9$ ) and do not much depend on the initial mass. Thus the increase of the rotation rate has qualitatively a similar effect on the location of the ZAMS as an increase of the initial metallicity. The ZAMS for non rotating models with twice the solar metallicity ( $Z = 0.040$ ) lies at a position which would

**Table 1.** Effect of rotation on the ZAMS

Initial mass	$\Omega/\Omega_{\text{crit}}$	$V_{\text{eq}}$ [km/sec]	Log $L/L_{\odot}$	Log $T_{\text{eff}}$	$\frac{R_p(\Omega)}{R_e(\Omega)}$	$\frac{R_e(\Omega)}{R_e(\Omega=0)}$
<b>9 <math>M_{\odot}</math> <math>\Omega_{\text{crit}} = 0.0001684</math> [sec<math>^{-1}</math>]</b>						
9 $M_{\odot}$	0.00	0.000	3.631	4.389	1.000	1.000
9	0.50	223.4	3.622	4.381	0.947	1.045
9	0.90	527.0	3.599	4.342	0.712	1.370
<b>20 <math>M_{\odot}</math> <math>\Omega_{\text{crit}} = 0.0001280</math> [sec<math>^{-1}</math>]</b>						
20 $M_{\odot}$	0.00	0.000	4.658	4.550	1.000	1.000
20	0.50	264.7	4.648	4.541	0.948	1.049
20	0.90	628.4	4.626	4.502	0.711	1.382
<b>40 <math>M_{\odot}</math> <math>\Omega_{\text{crit}} = 0.0000989</math> [sec<math>^{-1}</math>]</b>						
40 $M_{\odot}$	0.00	0.000	5.376	4.645	1.000	1.000
40	0.50	301.3	5.368	4.637	0.950	1.047
40	0.90	724.8	5.348	4.594	0.712	1.401
<b>60 <math>M_{\odot}</math> <math>\Omega_{\text{crit}} = 0.0000826</math> [sec<math>^{-1}</math>]</b>						
60 $M_{\odot}$	0.00	0.000	5.728	4.683	1.000	1.000
60	0.50	317.9	5.721	4.674	0.953	1.050
60	0.90	784.0	5.704	4.628	0.711	1.436

**Fig. 1.** Local effective temperatures as a function of the colatitude at the surface of 40  $M_{\odot}$  ZAMS models rotating at different velocities.

roughly corresponds to a value of  $\Omega/\Omega_{\text{crit}}$  equal to 0.7. The ZAMS internal structure of the star is little affected by rotation. The temperature profiles inside the three 40  $M_{\odot}$  ZAMS models presented in Table 1 differ by less than 5%.

**Fig. 2.** Upper ZAMS in the theoretical HR diagram for different rotation rates.

### 3.2. Hydrostatic effects of rotation on the main sequence

From the ZAMS presented above, models of 40 and 60  $M_{\odot}$  were evolved during the main sequence (MS) with account of only the hydrostatic effects and local conservation of the angular momentum. Some characteristics of the models are indicated in Table 2: the duration of the main sequence  $\tau_H$  is indicated in column 3, the position in the HR diagram at the end of the H-burning phase is given in columns 4 and 5, the central temperature and density at this stage are given in columns 6 and 7 respectively. As for the ZAMS models, the hydrostatic effects alone have a modest impact on the model outputs: when  $\Omega/\Omega_{\text{crit}}$  increases from 0 to 0.9, the lifetimes of the considered models are increased by 1 to 2%. The lifetime enhancement is a consequence of the decrease of the central temperature in rotating models due to the decreased effective gravity. The evolutionary tracks for the models with  $\Omega/\Omega_{\text{crit}} = 0.9$  are compared with the non rotating models in Fig. 3. The tracks are shifted towards lower luminosities. One can say roughly that a massive star having an initial rotational velocity equal to 90% of the critical velocity will have a behaviour similar to a non rotating star with an initial mass smaller by 0.5 to 2.5 solar masses.

Due to the envelope expansion which occurs during the main sequence, the surface equatorial velocity for the 40  $M_{\odot}$  model decreases by more than a factor three during this phase. The profile of the angular velocity at the end of the main sequence is presented in Fig. 4. The star has a radiative core at this stage with a steep angular velocity gradient. In the central regions, as a result of the core contraction, the angular velocity is enhanced by about a factor 30 with respect to the surface angular velocity.

### 4. Effects of the rotationally induced mixing

To study the effects of the rotationally induced mixing, we have computed a 40  $M_{\odot}$  model with  $\Omega/\Omega_{\text{crit}} = 0.9$ , including in addition to the hydrostatic effects discussed above, the effects of mixing of the chemical elements. The mixing of the chemical species, modelised through a diffusion equation in our rotating

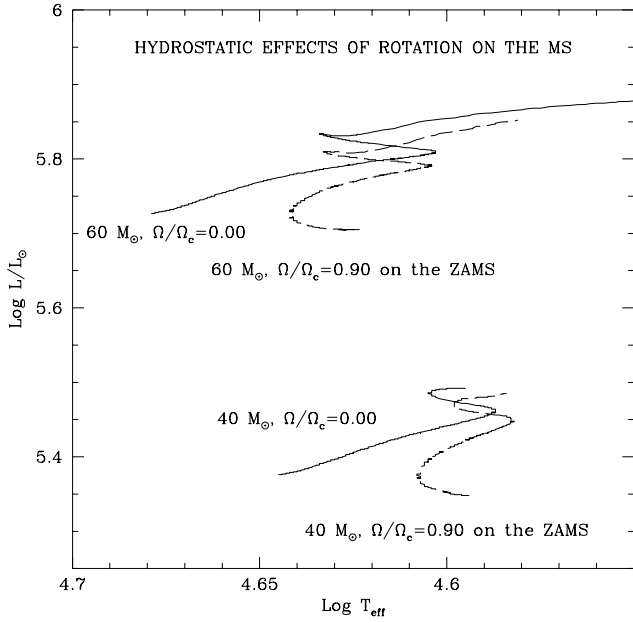


**Fig. 3.** Evolutionary tracks for 40 and 60  $M_{\odot}$  models for  $\Omega/\Omega_{\text{crit}} = 0$  and  $\Omega/\Omega_{\text{crit}} = 0.9$ .

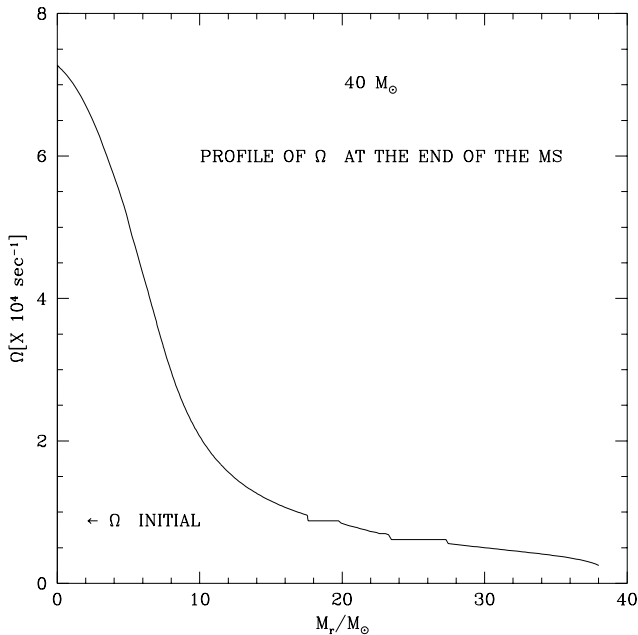


**Fig. 4.** Profile as a function of the Lagrangian mass coordinate of the angular velocity for the 40  $M_{\odot}$  model at the end of the main sequence. The arrow on the left of the figure indicates the initial value of the angular velocity ( $\Omega/\Omega_{\text{crit}} = 0.9$ ).

stellar models, intervenes through three hydrodynamical processes: the horizontal and vertical turbulence induced by the shear and the meridional circulation. The diffusion coefficient  $D_{\text{eff}}$ , which accounts for the effects of the horizontal turbulence induced by the shear and of the meridional circulation, exerts its effect whenever turbulent and circulation motions are sus-

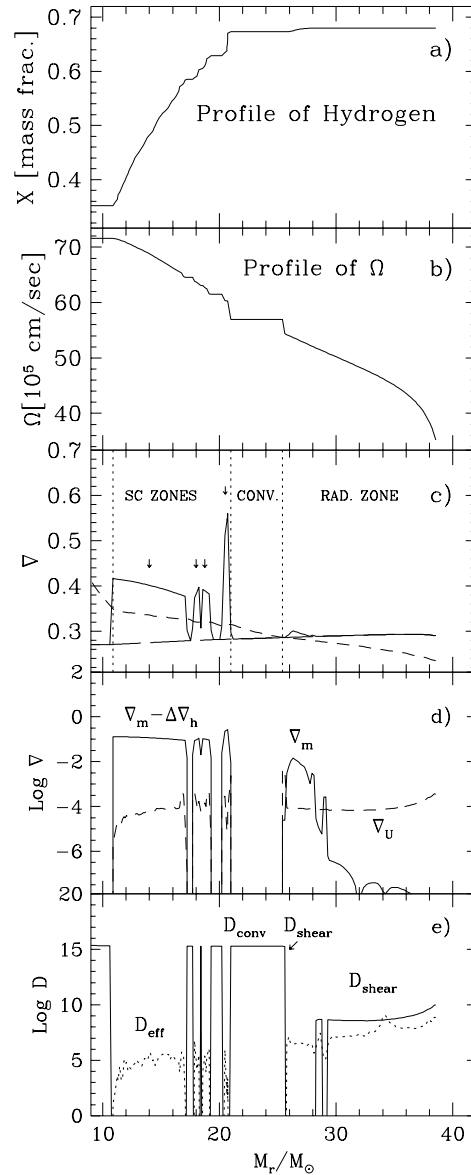


**Fig. 5a–e.** Profiles of various quantities inside a 40  $M_{\odot}$  stellar model during the H-burning phase: **a** Profile of the abundance of hydrogen (in mass fraction); **b** Profile of the angular velocity; **c** Profiles of  $\nabla_{\text{ad}} + \frac{\omega}{\delta} \nabla_{\mu}$  (continuous line), of  $\nabla_{\text{ad}}$  (long dashed line) and of  $\nabla_{\text{rad}}$  (short dashed line). In the zones where  $\nabla_{\mu}$  is zero,  $\nabla_{\text{ad}}$  is confounded with  $\nabla_{\text{ad}} + \frac{\omega}{\delta} \nabla_{\mu}$ ; **d** Profiles of  $\nabla_U$ ,  $\nabla_m$  and  $\nabla_m - \Delta \nabla_h$  (see text); **e** profiles of the diffusion coefficients  $D_{\text{shear}}$ ,  $D_{\text{eff}}$  and  $D_{\text{conv}}$ .

tained. The same is true for the action of  $D_{\text{shear}}$ , which describes the effects of the vertical turbulence induced by the shear. But its action is in addition submitted to the Richardson criterion which states when the shear is large enough to produce vertical mixing.

Let us recall that for a radiative zone, the Richardson stability criterion becomes (Maeder & Meynet 1996)

$$\nabla_U < \nabla_m, \quad (1)$$

**Table 2.** Effect of rotation on the MS

Initial mass	$\Omega/\Omega_{\max}$	$\tau_H$ [ $10^6$ yr]	Log L/ $L_{\odot}$ end of the MS	Log T <sub>eff</sub> end of the MS	Log T <sub>c</sub> end of the MS	Log $\rho_c$ end of the MS
40 $M_{\odot}$	0.00	3.1062	5.492	4.597	7.791	1.214
40	0.90	3.1693	5.479	4.593	7.775	1.201
60 $M_{\odot}$	0.00	2.7231	5.844	4.612	7.857	1.170
60	0.90	2.7572	5.810	4.629	7.829	1.122

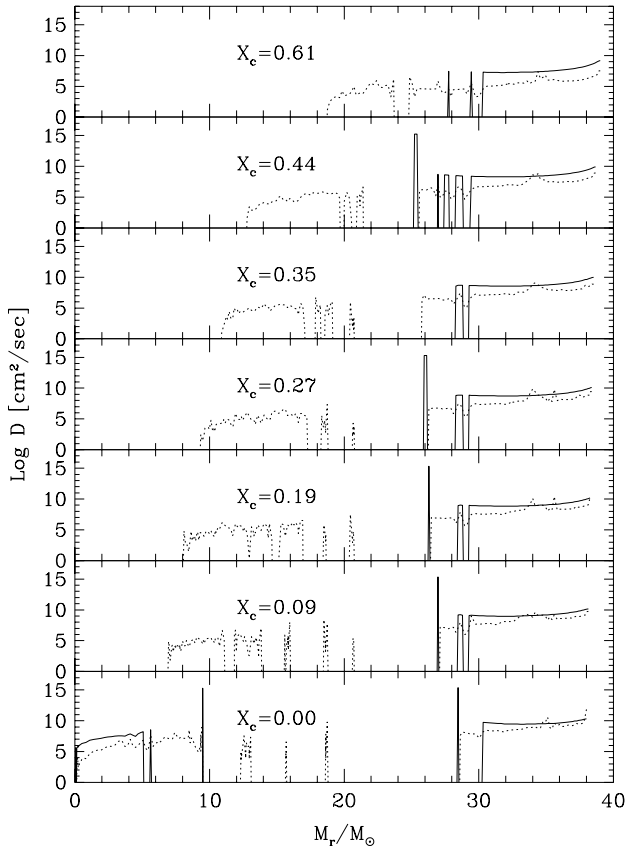


**Fig. 6.** Profiles at different stages during the main sequence of the diffusion coefficients in a 40  $M_{\odot}$  model computed with an initial  $\Omega = 0.9 \Omega_{\text{crit}}$ . Hydrostatic effects and rotationally induced mixing of the chemical species have been taken into account.  $X_c$  is the central mass fraction of hydrogen at the different stages considered.

where  $\nabla_U = \frac{1}{4} \frac{H_p}{g\delta} \left( \frac{dU}{dz} \right)^2$  and  $\nabla_m = \frac{\zeta}{\delta} \nabla_{\mu}$ , measure the strength of the shear and that of the  $\mu$ -gradient respectively. In a semiconvective zone, the stability criterion, with respect to shears, is

$$\nabla_U < \nabla_m - \Delta\nabla_h, \quad (2)$$

where  $\Delta\nabla_h = \frac{1}{1+2\sqrt{6}} (\nabla_{\text{rad}} - \nabla_{\text{ad}})$ . Current symbols are used (Kippenhahn & Weigert 1990, see also Maeder & Meynet 1996). On Fig. 5, we present the profiles of various physical quantities

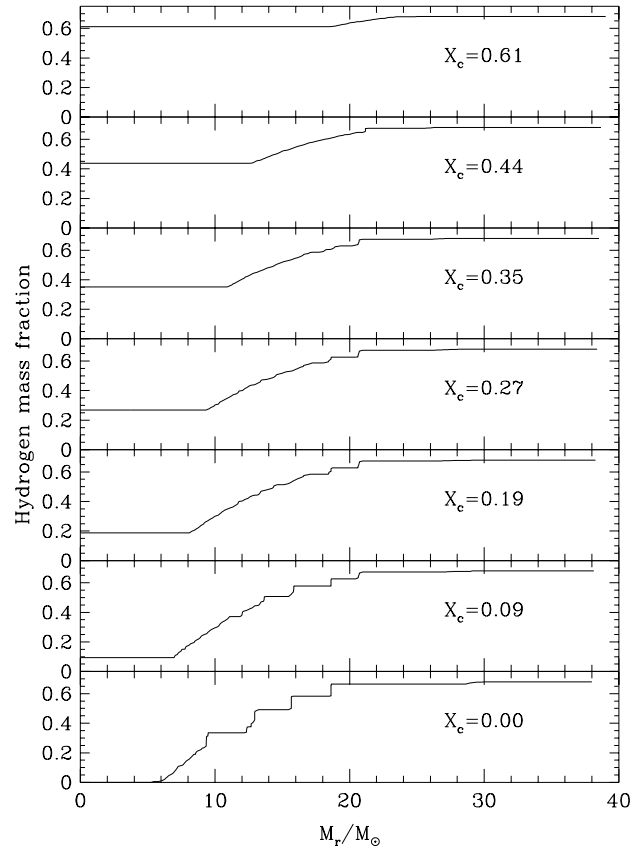


**Fig. 7.** Same as in Fig. 6 for the profiles of the abundance of hydrogen (in mass fraction).

inside the model with a hydrogen mass fraction at the centre equal to  $X_c = 0.35$ . Let us first concentrate on the semiconvective zone. We can note the following points:

1) The semiconvective zone encompasses nearly all the region where there is an important  $\mu$ -gradient just outside the convective core. (see panels a and c). Any efficient mixing in this zone would deeply affect the stellar structure.

2) In the semiconvective zones, the Richardson stability criterion is always fulfilled by a wide margin (see panel d). Indeed  $\nabla_m - \Delta\nabla_h$  ( $\sim 10^{-1}$ ) is 2-3 orders of magnitude greater than  $\nabla_U$  ( $\sim 10^{-4}$ ). Let us note that the term  $\Delta\nabla_h$  which, in a semi-

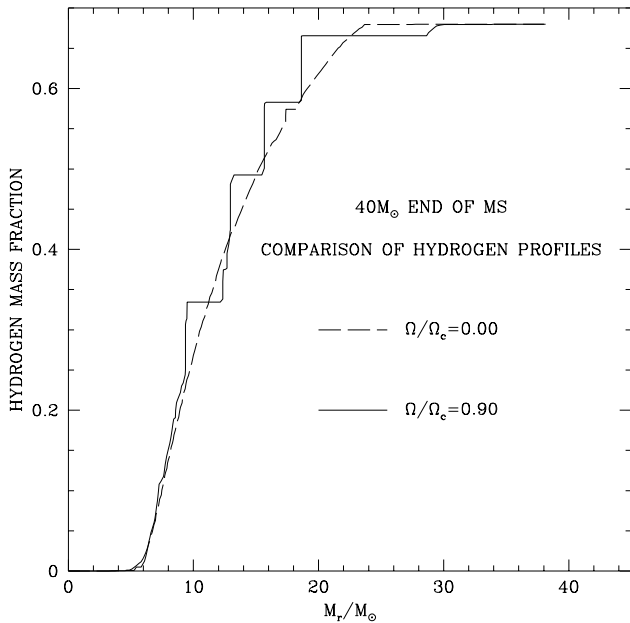


**Fig. 8.** Profiles of the mass fraction of hydrogen at the end of the main sequence in a  $40 M_{\odot}$  model computed with  $\Omega/\Omega_{\text{crit}} = 0.0$  (long dashed line) and  $\Omega/\Omega_{\text{crit}} = 0.9$  (continuous line). The hydrostatic effects of rotation and the rotationally induced mixing of the chemical species were considered in the rotating model.

convective zone, weakens the inhibiting effect of the  $\mu$ -gradient, has a negligible effect. Its value is of the order of  $10^{-2}$ .

3) The values of  $D_{\text{eff}}$  in this region range between  $10^5 - 10^6 \text{ cm}^2 \text{ s}^{-1}$ , implying a mixing timescale  $\tau_{\text{mix}} \sim R^2/D$  superior to  $10^9 \text{ y}$  ! ( $R$  is the radius of the star).

Thus, in a semiconvective zone, the vertical turbulence induced by the shear is never strong enough (by a wide margin) to overcome the inhibiting effects of the  $\mu$ -gradients. At the same time  $D_{\text{eff}}$  take too low values to produce a significant mixing.

Let us now turn to the radiative zone. One can see that:

1) In zones where  $\nabla_{\mu} \leq 10^{-4}$ ,  $D_{\text{shear}}$  can reach values as high as  $10^9 - 10^{10} \text{ cm}^2 \text{ s}^{-1}$ . For such values the mixing timescale is of the order of  $10^6 \text{ y}$ , *i.e.* shorter than the main sequence lifetime. But, this occurs in zones where there is almost nothing to mix, the regions being already nearly completely homogeneous.

2) At the base of this radiative zone, the chemical profile steepens and  $\nabla_m$ , which can reach values as high as  $10^{-2}$ , stabilizes the medium.

3) Only in the small zone of very strong  $\Omega$ -gradient and of  $\mu$ -gradient nearly zero, which occurs above the main intermediate convective zone (at  $M_r$  between 25 and  $26 M_{\odot}$ ) does the shear overcome again the  $\mu$ -barrier. In this zone, the critical parameter  $\theta$  defined by Maeder & Meynet (1996) is inferior to  $\frac{-1}{1+2\sqrt{6}}$ . In that case there is no preferred turbulent scale which can be used to define the diffusion coefficient and we choose to set the diffusion coefficient equal to the convective diffusion coefficient as it can be expressed in the frame of the mixing length theory.

A posteriori this procedure seems justified. Indeed the zones where this situation occurs are always adjacent to a convective zone and the peak which appear on Fig. 5, panel e) (see also Fig. 6), can be seen as a small extension of an adjacent convective zone.

4) In the radiative regions, the values of  $D_{\text{eff}}$  are generally one or two orders of magnitude lower than that of  $D_{\text{shear}}$  in agreement with the expectations of Zahn (1992).

To resume, in radiative zones, the diffusion coefficients are strong enough to produce an efficient mixing only in regions where there is almost nothing to mix.

The same situations occur during the whole H-burning phase. Comparing Figs. 6 and 7 which show the profiles of the diffusion coefficients and of the hydrogen in seven models during the H-burning phase, one immediately sees that where  $\mu$ -gradients are present, *i.e.* in regions where an efficient mixing would have the strongest impact, the diffusion coefficient  $D_{\text{shear}}$  is zero ! As explained above, the peaks of  $D_{\text{shear}}$  are small extensions of adjacent convective zones (see Fig. 5 panel e).

From these considerations, one can conclude that the rotationally induced mixing will have a very limited impact on the chemical profiles and subsequently on the stellar structure. This is indeed the case. On Fig. 8 the profile of the hydrogen mass fraction, at the end of the MS, inside the stellar model obtained with rotationally induced mixing, is compared with the one in the standard model (without rotation). The action of  $D_{\text{eff}}$  in the rotating model gives birth to a series of intermediate convective zones which are nearly totally absent in the standard model. Apart from these differences the general shapes of the two profiles are quite similar. In particular, the sizes of the convective cores are the same and no significant changes of the surface abundances are observed in the rotating model. The main sequence lifetimes of the two models differ by less than 0.4%. The similarity of the two models is a consequence of the very strong inhibiting effect of the  $\mu$ -gradient. Indeed the condition for mixing (very low  $\mu$ -gradient) prevents the mixing to have an important impact (in strong  $\mu$ -gradient regions)!

Let us note that this conclusion on the inhibiting effect of the  $\mu$ -gradient is reinforced by the fact that we did not consider here any transport mechanism of the angular momentum. Indeed, had we done so, the angular velocity gradients would likely have been smoothed and the shear would have been weaker than in the present model. Let us also mention that the choice of another criterion for the convection has no impact on this conclusion. Indeed if the Schwarzschild criterion had been chosen instead of the Ledoux criterion, this would have simply shifted the region of the  $\mu$ -gradient outwards without removing its inhibiting effect on the turbulent mixing. Thus we are left with the conclusion that even with very high initial angular velocity (here 90% of the critical velocity on the ZAMS), no rotational mixing is expected to occur during the main sequence of a massive star. Although this result confirms previous theoretical investigations which have also shown the strong inhibiting effect of the  $\mu$ -gradients (Chaboyer et al. 1995), we cannot be fully happy with it. Indeed this result does not account for the observations

of Herrero et al. (1992) which show that mixing by rotation is strong enough to operate on timescales shorter than the main sequence lifetime. Thus we consider the above results not as a proof of the inefficiency of rotational mixing but as a sign that some processes are still inadequately described by theory.

## 5. Conclusions

The main results of this paper are summarized in the abstract and will not be repeated here. Let us however make a few comments on the need of further improvements of the theory.

First let us recall that the inhibiting nature of the  $\mu$ -gradient is linked to its presence in the Richardson criterion. Would there be no Richardson criterion, there would be no  $\mu$ -gradient inhibiting effect. However we are not allowed to neglect the Richardson criterion. Indeed the Richardson criterion tells us when there is sufficient energy in the shear to allow mixing. If we must keep the Richardson criterion, we can however wonder if its formulation is not too schematic. In particular, its derivation does not account for the other already existing milder sources of turbulence such as semiconvection and horizontal turbulence (cf. Zahn 1992), which may be present even when Richardson criterion says there is no turbulence. This pre-existing mild turbulence would make invalid some of the usual assumptions as for example the assumption of full homogeneity at any level and also the usual assumption that the turbulent eddies keep their original composition. Thus we come to the conclusion that the progress of stellar modeling may only go through a better hydrodynamical description of turbulence.

## Appendix A

Although the Kippenhahn & Thomas (1970) method is applicable only in conservative cases (see section 2), most authors use it to treat the case of a “shellular rotation law” (clearly a non conservative case) without checking the conditions under which such a procedure is possible. Here we bring some clarifications on the implicit assumptions made when the the Kippenhahn & Thomas method is used in the case of a “shellular rotation law”.

### A.1 The interior stellar structure equations

Let us show that for a “shellular rotation law” the surfaces  $\Psi_P$  given by the equation

$$\Psi_P = \Phi + \frac{1}{2}\Omega^2 r^2 \sin^2 \theta = \text{constant} \quad (\text{A.1})$$

are isobars.  $\Phi = -V$ , where  $V$  is the gravitational potential,  $r$  is the radius,  $\Omega$  the angular rotation rate and  $\theta$  the colatitude.

The hydrostatic equilibrium implies that

$$\vec{\nabla} P = -\rho \vec{g}_{\text{eff}}$$

where  $\vec{g}_{\text{eff}}$  is the effective gravity. In spherical coordinates, its components write

$$g_{\text{eff},r} = \frac{\partial \Phi}{\partial r} + \Omega^2 r \sin^2 \theta, \quad (\text{A.2})$$

$$g_{\text{eff},\theta} = \frac{1}{r} \frac{\partial \Phi}{\partial \theta} + \Omega^2 r \sin \theta \cos \theta. \quad (\text{A.3})$$

The components of the gradient of  $\Psi_P$  in polar coordinates  $r$ ,  $\theta$  are

$$\frac{\partial \Psi_P}{\partial r} = \frac{\partial \Phi}{\partial r} + \Omega^2 r \sin^2 \theta + r^2 \sin^2 \theta \Omega \frac{\partial \Omega}{\partial r}, \quad (\text{A.4})$$

$$\frac{1}{r} \frac{\partial \Psi_P}{\partial \theta} = \frac{1}{r} \frac{\partial \Phi}{\partial \theta} + \Omega^2 r \sin \theta \cos \theta + r^2 \sin^2 \theta \Omega \frac{1}{r} \frac{\partial \Omega}{\partial \theta}. \quad (\text{A.5})$$

Comparing (A.4) with (A.2) and (A.5) with (A.3), one can write

$$\vec{g}_{\text{eff}} = \vec{\nabla} \Psi_P - r^2 \sin^2 \theta \Omega \vec{\nabla} \Omega. \quad (\text{A.6})$$

Thus the expression for the hydrostatic equilibrium may be written

$$\vec{\nabla} P = -\rho(\vec{\nabla} \Psi_P - r^2 \sin^2 \theta \Omega \vec{\nabla} \Omega). \quad (\text{A.7})$$

Since  $\Omega$  is constant on the isobars, the vector  $\vec{\nabla} \Omega$  is parallel to the vector  $\vec{\nabla} P$ . The hydrostatic equation (A.7) implies then that  $\vec{\nabla} P$  is parallel to  $\vec{\nabla} \Psi_P$ . Therefore the surfaces defined by  $\Psi_P = \text{constant}$  correspond to isobaric surfaces and this ends the demonstration. It is interesting to note that the shape of the isobars in the case of a “shellular rotation law” are identical to the shape of the equipotentials in a conservative situation.

Once the shape of the isobars is known, one can write the stellar structure equations on these isobars. In the following we shall drop the subscript  $P$  attached to  $\Psi$  and the symbol  $g$  will be used instead of  $g_{\text{eff}}$ . Following the method of Kippenhahn & Thomas we define  $r_P$  by

$$V_P = \frac{4\pi}{3} r_P^3,$$

where  $V_P$  is the volume inside an isobar. For any quantity,  $q$ , which is not constant over an isobaric surface, a mean value is defined by

$$\langle q \rangle = \frac{1}{S_P} \int_{\Psi=\text{const}} q d\sigma,$$

where  $S_P$  is the surface of the isobar and  $d\sigma$  is an element of that surface.

#### A.1.1 Hydrostatic equilibrium equation

The effective gravity can no longer be defined by  $g = \frac{d\Psi}{dn}$  ( $g \equiv \|\vec{g}\|$  and  $\frac{d\Psi}{dn} \equiv \|\vec{\nabla} \Psi\|$ ), since  $\Psi$  is not a potential ( $dn$  is the distance between two neighboring isobaric surfaces  $\Psi=\text{const}$ . and  $\Psi + d\Psi=\text{const}$ .). Let us use the fact that  $\vec{\nabla} \Omega$  is parallel to  $\vec{\nabla} \Psi$  and thus can be expressed by  $\vec{\nabla} \Omega = \alpha \vec{\nabla} \Psi$  with  $\alpha = \frac{d\Omega}{d\Psi}$  a scalar which depends only on  $\Psi$ . Replacing  $\vec{\nabla} \Omega$  by this expression as a function of  $\vec{\nabla} \Psi$  in A.7 leads to the following expression for the effective gravity

$$g = (1 - r^2 \sin^2 \theta \Omega \alpha) \frac{d\Psi}{dn},$$

which implies that

$$\frac{dn}{d\Psi} = \frac{(1 - r^2 \sin^2 \theta \Omega \alpha)}{g}. \quad (A.8)$$

The hydrostatic equation then writes

$$\frac{dP}{dn} = -\rho(1 - r^2 \sin^2 \theta \Omega \alpha) \frac{d\Psi}{dn},$$

or

$$\frac{dP}{d\Psi} = -\rho(1 - r^2 \sin^2 \theta \Omega \alpha). \quad (A.9)$$

From this equation, one can immediately deduce that the quantity  $\rho(1 - r^2 \sin^2 \theta \Omega \alpha)$  is constant on an isobar.

In order to have  $M_P$ , *i.e.* the mass inside the isobar, as independent variable, one has to find the expression for  $\frac{d\Psi}{dM_P}$ . One can write, using (A.8)

$$\begin{aligned} dM_P &= \int_{\Psi=\text{const}} \rho dn d\sigma = d\Psi \int_{\Psi=\text{const}} \rho \frac{dn}{d\Psi} d\sigma \\ &= d\Psi \int_{\Psi=\text{const}} \rho \frac{(1 - r^2 \sin^2 \theta \Omega \alpha)}{g} d\sigma. \end{aligned} \quad (A.10)$$

The fact that  $\rho(1 - r^2 \sin^2 \theta \Omega \alpha)$  is constant on an isobar leads to

$$\frac{d\Psi}{dM_P} = \frac{1}{\rho(1 - r^2 \sin^2 \theta \Omega \alpha) \langle g^{-1} \rangle S_P}. \quad (A.11)$$

Thus, using (A.9) and (A.11),

$$\frac{dP}{dM_P} = \frac{dP}{d\Psi} \frac{d\Psi}{dM_P} = \frac{-1}{\langle g^{-1} \rangle S_P}.$$

Setting

$$f_P = \frac{4\pi r_P^4}{GM_P S_P} \frac{1}{\langle g^{-1} \rangle}, \quad (A.12)$$

$G$  being the gravitational constant, the hydrostatic equilibrium equation writes

$$\frac{dP}{dM_P} = -\frac{GM_P}{4\pi r_P^4} f_P. \quad (A.13)$$

Thus expressed in terms of the lagrangian variable  $M_P$ , the hydrostatic equation keeps the same form as in the conservative case.

### A.1.2 Conservation of the mass

The volume of a shell comprised between two isobars is by definition of  $r_P$

$$dV_P = 4\pi r_P^2 dr_P. \quad (A.14)$$

It can also be expressed by

$$dV_P = \int_{\Psi=\text{const}} dn d\sigma = d\Psi \int_{\Psi=\text{const}} \frac{dn}{d\Psi} d\sigma$$

$$= d\Psi \int_{\Psi=\text{const}} \frac{(1 - r^2 \sin^2 \theta \Omega \alpha)}{g} d\sigma,$$

which finally gives

$$dV_P = d\Psi S_P \left[ \langle g^{-1} \rangle - \langle g^{-1} r^2 \sin^2 \theta \rangle \Omega \alpha \right]. \quad (A.15)$$

From (A.14) and (A.15), one can deduce  $dr_P/d\Psi$  and, using (A.11), one obtains

$$\frac{dr_P}{dM_P} = \frac{1}{4\pi r_P^2 \bar{\rho}}, \quad (A.16)$$

where

$$\bar{\rho} = \frac{\rho(1 - r^2 \sin^2 \theta \Omega \alpha) \langle g^{-1} \rangle}{\langle g^{-1} \rangle - \langle g^{-1} r^2 \sin^2 \theta \rangle \Omega \alpha}. \quad (A.17)$$

Let us note that  $\bar{\rho}$  is not equal to  $\langle \rho \rangle$ . Indeed  $\bar{\rho}$  is obtained by averaging the density over the volume between two isobars, instead  $\langle \rho \rangle$  is an average performed on an isobaric surface.

### A.1.3 Conservation of the energy

One can write that the net energy outflow from a shell comprised between the isobars  $\Psi$  and  $\Psi + d\Psi$  is equal to

$$dL_P = \int_{\Psi=\text{const}} \epsilon \rho dn d\sigma = d\Psi \int_{\Psi=\text{const}} \epsilon \rho \frac{dn}{d\Psi} d\sigma,$$

where  $\epsilon$  is the net rate of energy production in the shell. Using (A.8) and the constancy of  $\rho(1 - r^2 \sin^2 \theta \Omega \alpha)$  on an isobar, one can write

$$dL_P = d\Psi \langle \frac{\epsilon}{g} \rangle S_P \rho(1 - r^2 \sin^2 \theta \Omega \alpha). \quad (A.18).$$

Using expression (A.11), one finally obtains decomposing  $\epsilon$  into its nuclear, gravitational and neutrino components,

$$\frac{dL_P}{dM_P} = \frac{\langle (\epsilon_{nucl} - \epsilon_\nu + \epsilon_{grav}) g^{-1} \rangle}{\langle g^{-1} \rangle}. \quad (A.19)$$

### A.1.4 Radiative equilibrium

Locally, the equation of radiative transfer writes

$$F = -\frac{4acT^3}{3\kappa\rho} \frac{dT}{dn}, \quad (A.20)$$

where  $F$  is the radiative flux at a given point on the isobar. Using the fact that  $\frac{dT}{dn} = \frac{dT}{dM_P} \frac{dM_P}{d\Psi} \frac{d\Psi}{dn}$  and the expressions (A.8) and (A.11), one has that

$$F = -\frac{4acT^3}{3\kappa\rho} \frac{dT}{dM_P} \rho \langle g^{-1} \rangle S_P g.$$

Integrating over an isobar, one obtains

$$L_P = -\frac{4ac}{3} \langle g^{-1} \rangle S_P^2 \langle \frac{T^3 g}{\kappa} \frac{dT}{dM_P} \rangle. \quad (A.21)$$

### A.1.5 Convective transport

In a convective region one has that locally, *i.e.* at a given point on an isobar,

$$\frac{d \ln T}{d \ln p} = \nabla_{\text{ad}}.$$

Taking the averages on an isobar of the both sides of this equality, implies that

$$\left\langle \frac{d \ln T}{d \ln p} \right\rangle = \left\langle \nabla_{\text{ad}} \right\rangle. \quad (\text{A.22})$$

### A.1.6 Simplifying assumptions

From the equations presented above, one can see that because of the non constancy of the density and temperature on isobars in the case of a “shellular rotation law”, it is not possible to write as simple equations as in the conservative case. However let us see under which conditions one can transform the equations (A.13), (A.16), (A.19), (A.21) and (A.22) into the form proposed by Kippenhahn & Thomas (1970).

First, from equation (A.16), one immediately sees that if, instead of  $\rho$ , one considers as a dependant variable the quantity  $\bar{\rho}$ , the continuity equation for the mass keeps its usual form. We shall consider also a mean temperature  $\bar{T}$  obtained from the equation of state with as input variables  $\bar{\rho}$ ,  $p$  and the chemical composition. The chemical composition is supposed to be homogeneous on an isobaric surface due to the strong horizontal turbulence. The energy conservation equation and the energy transport equation are written using these mean values of the density and the temperature, making the following approximations:

$$\begin{aligned} & \left\langle (\epsilon_{\text{nucl}} - \epsilon_{\nu} + \epsilon_{\text{grav}}) g^{-1} \right\rangle / \left\langle g^{-1} \right\rangle \\ & \approx \epsilon_{\text{nucl}}(\bar{\rho}, \bar{T}) - \epsilon_{\nu}(\bar{\rho}, \bar{T}) + \epsilon_{\text{grav}}(\bar{\rho}, \bar{T}), \end{aligned} \quad (\text{A.23})$$

$$\left\langle \frac{T^3 g}{\kappa} \frac{dT}{dM_P} \right\rangle \approx \frac{\bar{T}^3}{\kappa(\bar{\rho}, \bar{T})} \left\langle g \right\rangle \frac{d\bar{T}}{dM_P}, \quad (\text{A.24})$$

$$\left\langle \frac{d \ln T}{d \ln p} \right\rangle \approx \frac{d \ln \bar{T}}{d \ln p}, \quad (\text{A.25})$$

and

$$\left\langle \nabla_{\text{ad}} \right\rangle \approx \nabla_{\text{ad}}(\bar{\rho}, \bar{T}). \quad (\text{A.26})$$

With these changes of variables and these approximations we recover the set of stellar structure equations given by Kippenhahn & Thomas (1970), *i.e.*:

$$\frac{\partial P}{\partial M_P} = - \frac{GM_P}{4\pi r_P^4} f_P, \quad (\text{A.27})$$

$$\frac{\partial r_P}{\partial M_P} = \frac{1}{4\pi r_P^2 \bar{\rho}}, \quad (\text{A.28})$$

$$\frac{\partial L_P}{\partial M_P} = \epsilon_{\text{nucl}} - \epsilon_{\nu} + \epsilon_{\text{grav}}, \quad (\text{A.29})$$

$$\frac{\partial \ln T}{\partial M_P} = - \frac{GM_P}{4\pi r_P^4} f_P \min[\nabla_{\text{ad}}, \nabla_{\text{rad}} \frac{f_T}{f_P}], \quad (\text{A.30})$$

where

$$f_P = \frac{4\pi r_P^4}{GM_P S_P} \frac{1}{\left\langle g^{-1} \right\rangle}, \quad (\text{A.31})$$

$$f_T = \left( \frac{4\pi r_P^2}{S_P} \right)^2 \frac{1}{\left\langle g \right\rangle \left\langle g^{-1} \right\rangle}. \quad (\text{A.32})$$

Partial derivatives have replaced total derivatives to allow for the fact that the quantities depend not only on  $M_P$  but also on time. Let us note here that the simplifying assumptions (A.23) to (A.26) do not appear too severe. First we have shown that the equations describing the hydrostatic equilibrium and the conservation of mass are strictly valid in the case of a “shellular rotation law”, provided that  $\bar{\rho}$  is considered as the dependant variable for the density. Moreover the strong horizontal turbulence responsible for the constancy of  $\Omega$  on isobars will likely homogenize the chemical composition and reduce the constrasts in densities and temperatures on isobars, making the above approximations justified. In the present computation we used the Roche model for the computation of the gravitational potential.

## A.2 The equations for the stellar envelope

We call envelope (cf. Kippenhahn et al. 1967) the layers connecting the inner solutions to the atmosphere. In the envelope, convection is treated non adiabatically, partial ionisation is treated in details and the  $\epsilon$ 's are considered to be zero. The envelopes of massive hot stars contain only a few thousands of the total mass, thus we may consider that the envelope rotates with a uniform angular velocity equal to that of the first (outermost) interior shell. In that case we have locally a solid rotation law. The independant variable  $M_P$ , used in the interior is advantageously replaced by the pressure which in the outer parts of the star covers a much wider range of values. Using the pressure as the independant variable, the equations of stellar structure become:

$$\frac{\partial \ln r_P}{\partial \ln P} = \frac{P}{r_P} \frac{\partial r_P}{\partial M_P} \frac{\partial M_P}{\partial P} = - \frac{r_P P}{GM_P \bar{\rho}} \frac{1}{f_P}, \quad (\text{A.33})$$

$$\frac{\partial \ln M_P}{\partial \ln P} = \frac{P}{M_P} \frac{\partial M_P}{\partial P} = - \frac{4\pi r_P^4 P}{GM_P^2} \frac{1}{f_P}, \quad (\text{A.34})$$

$$\frac{\partial \ln T}{\partial \ln P} = \min[\nabla_{\text{conv}}, \nabla_{\text{rad}} \frac{f_T}{f_P}]. \quad (\text{A.35})$$

### A.3 The equations for the atmosphere

In the atmosphere, the mass, the radius and the luminosity are supposed to keep constant values. Only the hydrostatic equilibrium equation and the radiative transfer equations must be solved. We shall suppose that  $\Omega$  is constant as a function of the depth and take the same value as in the envelope. In this case, the effective gravity can be derived from a potential and one can write (see eq. A.9)

$$\frac{dP}{d\Psi} = -\rho.$$

Using the fact that  $\frac{dr_P}{d\Psi} = \frac{S_P \langle g^{-1} \rangle}{4\pi r_P^2}$  (see expressions (A.14) and (A.15), with  $\alpha = \frac{d\Omega}{d\Psi} = 0$ ), one has that

$$\frac{dP}{dr_P} = \frac{dP}{d\Psi} \frac{d\Psi}{dr_P} = -\rho \frac{4\pi r_P^2}{S_P \langle g^{-1} \rangle}.$$

Defining the optical depth by  $d\tau_P = -\kappa \rho dr_P$ , one obtains

$$\frac{dP}{d\tau_P} = \frac{1}{\kappa} \frac{4\pi r_P^2}{S_P \langle g^{-1} \rangle},$$

which can be transformed into

$$\frac{d\tau_P}{d \log_{10} P} = \kappa \frac{S_P \langle g^{-1} \rangle}{4\pi r_P^2} P \ln 10. \quad (\text{A.36})$$

The equation of radiative equilibrium may be transformed into a relation linking the temperature to the optical depth. Let us call  $P_{\text{rad}}$  the radiation pressure. One can write

$$\frac{dP_{\text{rad}}}{dn} = \frac{dP_{\text{rad}}}{d\Psi} \frac{d\Psi}{dn} = \frac{dP_{\text{rad}}}{dr_P} \frac{dr_P}{d\Psi} g.$$

Since  $\frac{dr_P}{d\Psi} = \frac{S_P \langle g^{-1} \rangle}{4\pi r_P^2}$ , one obtains

$$\frac{dP_{\text{rad}}}{dn} = \frac{dP_{\text{rad}}}{dr_P} \frac{S_P \langle g^{-1} \rangle}{4\pi r_P^2} g. \quad (\text{A.37})$$

On the other hand, in the diffusive approximation, one can write locally at  $r_P$

$$\frac{dP_{\text{rad}}}{dn} = -\frac{\kappa \rho}{c} F. \quad (\text{A.38})$$

Together with the expression (A.37), one obtains

$$\frac{dP_{\text{rad}}}{dr_P} = -\frac{4\pi r_P^2}{S_P \langle g^{-1} \rangle} \frac{\kappa \rho}{c} \frac{F}{g}. \quad (\text{A.39})$$

Using the expression for the optical depth given above, one has that

$$\frac{dP_{\text{rad}}}{d\tau_P} = \frac{4\pi r_P^2}{S_P \langle g^{-1} \rangle} \frac{1}{c} \frac{F}{g}.$$

Integrating from  $\tau_P$  to the surface

$$P_{\text{rad}}(\tau_P) = \frac{4\pi r_P^2}{S_P \langle g^{-1} \rangle} \frac{1}{c} \frac{F}{g} \tau_P + P_{\text{rad}}(0).$$

In the case the specific intensity can be considered as isotropic and as having non zero value only in the outward direction, one has that

$$\frac{cP_{\text{rad}}(0)}{F} = 2/3.$$

Thus one can write

$$P_{\text{rad}}(\tau_P) = \frac{F}{gc} \left[ \frac{4\pi r_P^2}{S_P \langle g^{-1} \rangle} \tau_P + 2/3 g \right].$$

Now the theorem of von Zeipel (1924) enables ones to write

$$\frac{F}{g} = \text{const} = \frac{L}{S_P \langle g \rangle}.$$

Thus

$$P_{\text{rad}} = \frac{L}{S_P \langle g \rangle c} \left[ \frac{4\pi r_P^2}{S_P \langle g^{-1} \rangle} \tau_P + 2/3 g \right].$$

Let us define  $T_{\text{eff}}$  by the expression  $L = S_P \sigma T_{\text{eff}}^4$ . Then

$$P_{\text{rad}} = \frac{S_P \sigma T_{\text{eff}}^4}{S_P \langle g \rangle c} \left[ \frac{4\pi r_P^2}{S_P \langle g^{-1} \rangle} \tau_P + 2/3 g \right].$$

With  $P_{\text{rad}} = \frac{4}{3} \frac{\sigma}{c} T^4$ , and introducing the expression A.32 for  $f_T$  one finally obtains

$$T^4(\tau_P) = \frac{3}{4} T_{\text{eff}}^4 \left[ \frac{S_P}{4\pi r_P^2} f_T \tau_P + \frac{2}{3} \frac{g}{\langle g \rangle} \right]. \quad (\text{A.40})$$

### A.4 The equation for the local conservation of the angular momentum

Actually, one should resolve an equation of transfer for the angular momentum. However in the case of “no wind” and for asymptotic regime, the advection of angular momentum by the meridional currents are compensated by the diffusion of angular momentum through shear flow (cf. Zahn 1992). Thus one can consider that the angular momentum per unit mass in a given shell remains constant with time.

The momentum of inertia  $dI$  of a shell comprised between two isobars is

$$dI = \int_{S_P} r^2 \sin^2 \theta \rho dn d\sigma = \int_{S_P} r^2 \sin^2 \theta \rho \frac{dn}{d\Psi} d\Psi d\sigma.$$

Using (A.8) and the constancy of  $\rho(1 - r^2 \sin^2 \theta \Omega \alpha)$  on an isobar, one can write

$$dI = \rho(1 - r^2 \sin^2 \theta \Omega \alpha) d\Psi S_P \langle g^{-1} r^2 \sin^2 \theta \rangle.$$

With (A.11) this gives

$$dI = \frac{\langle g^{-1} r^2 \sin^2 \theta \rangle}{\langle g^{-1} \rangle} dM_P.$$

Since  $\Omega$  is constant on an isobar, the angular momentum,  $dG$ , can be written

$$dG = \Omega dI = \Omega \frac{\langle g^{-1} r^2 \sin^2 \theta \rangle}{\langle g^{-1} \rangle} dM_P.$$

Thus, the angular momentum per unit of mass for a given shell comprised between two isobars is given by

$$G_m = \frac{\Omega \langle g^{-1} r^2 \sin^2 \theta \rangle}{\langle g^{-1} \rangle}. \quad (\text{A.41})$$

## References

- Chaboyer B., Demarque P., Pinsonneault M.H., 1995, ApJ 441, 865
- Chandrasekhar S. 1961, Hydrodynamic and Hydromagnetic Stability, Clarendon Press, Oxford, p. 491
- Charbonnel C., 1994, A&A 282, 811
- Charbonnel C., 1995, ApJ 453, L41
- Dahmen G., Wilson T.L., Matteucci F., 1995, A&A 295, 194
- Eddington A.S., 1925, Observatory 48, 78
- Eddington A.S., 1926, The Internal Constitution of the Stars (repr. 1959 Dover; New York)
- Endal A.S., Sofia S., 1976, ApJ 210, 184
- Faulkner J., Roxburgh I.W., Strittmatter, P.A., 1968, ApJ 151, 203
- Fitzpatrick E.L., Garmany C.D., 1990, ApJ 363, 119
- Fliegner J., Langer N., 1995, in: Wolf-Rayet Stars: Binaries, Colliding Winds, Evolution, IAU Symp. 163, K.A. van der Hucht and P.M. Williams (eds.), Kluwer, p. 326
- Fransson C., Cassatella A., Gilmozzi R., Kirshner R.P., Panagia N. et al., 1989, ApJ 336, 429
- Herrero A., Kudritzki R.P., Vilchez J.M., Kunze D., Butler K., Haser S., 1992, A&A 261, 209
- Iglesias C.A., Rogers F.J., 1993, ApJ 412, 752
- Kippenhahn R., 1977, A&A 58, 267
- Kippenhahn R., Meyer-Hofmeister E., Thomas H.-C., 1970, A&A 5, 155
- Kippenhahn R., Thomas H.-C., 1970, in: Stellar Rotation, IAU Coll. 4, Ed. A. Slettebak, 20
- Kippenhahn R., Weigert A., 1990, Stellar Structure and Evolution, Springer Verlag, p. 426
- Kippenhahn R., Weigert A., Hofmeister E., 1967, Methods in Computational Physics 7, 129
- Kunth D., Matteucci F., Marconi G., 1995, A&A 297, 634
- Kurucz R.L., 1991, in: Stellar Atmospheres: Beyond Classical Models, NATO ASI Series C, Vol. 341, Eds. L.Crivellari, I.Hubeny, D.G.Hummer, p. 441
- Langer N., 1991, A&A 248, 531
- Langer N., Maeder A. 1995, A&A 295, 685
- Maeder A., 1971, PhD thesis, Geneva Observatory
- Maeder A., 1995a, A&A 299, 84
- Maeder A., 1995b, in *Astrophysical Applications of Stellar Pulsation*, IAU Coll. 155, Stobie R.S & Whitelock P.A. (Eds), ASP Conf Ser. 83, p.1
- Maeder A., Meynet G., 1989, A&A 210, 155
- Maeder A., Meynet G., 1996, A&A 313, 140
- Mowlavi N., 1995, PhD thesis, U.L.B., Bruxelles
- Pinsonneault M.H., Kawaler S.D., Demarque P., 1990, ApJS 74, 501
- Sackmann I.-J., 1970, A&A 8, 76
- Schaller G., Schaerer D., Meynet G., Maeder A., 1992, A&AS 96, 269
- Spiegel E.A., Zahn J.-P., 1970, Comments Astrophys. Space Phys. 2, 178
- Tassoul J.L., 1978, Theory of Rotating Stars, J.P. Ostriker (Ed.), Princeton Series in Astrophysics, Princeton
- Tomczyk S., Schou J., Thomson M.J., 1995, ApJ 448, L57
- Venn K.A., 1995a, ApJ 449, 839
- Venn K.A., 1995b, ApJS 99, 659
- Venn K.A., Lambert D.L., Lemke M., 1996, A&A 307, 849
- Vogt H., 1925, Astron. Nachr. 223, 229
- von Zeipel, H., 1924, MNRAS 84, 665
- Walborn N.R., 1976, ApJ 205, 419
- Zahn J.-P., 1974, in: Stellar Instability and Evolution, IAU Symp. 59, P. Ledoux et al. (Eds.), Reidel, p. 185
- Zahn J.-P., 1975, Mém. Soc. Roy. Sci. Liège, 6e série 8, 31
- Zahn J.-P., 1992, A&A 265, 115

This article was processed by the author using Springer-Verlag L<sup>A</sup>T<sub>E</sub>X A&A style file L-AA version 3.